AMERICAN SOCIETY FOR MICROBIOLOGY | mBio®

RESEARCH ARTICLE
Molecular Biology and Physiology

Topoisomerase 2β Induces DNA Breaks To Regulate Human Papillomavirus Replication

Paul Kaminski,[a] Shiyuan Hong,[a,b] Takeyuki Kono,[a] Paul Hoover,[a] Laimonis Laimins[a]

[a]Department of Microbiology-Immunology, Northwestern University, Feinberg School of Medicine, Chicago, Illinois, USA
[b]Institute of Life Sciences, Chongqing Medical University, Chongqing, China

Paul Kaminski and Shiyuan Hong contributed equally to this work. Author order was determined in order of increasing seniority.

ABSTRACT Topoisomerases regulate higher-order chromatin structures through the transient breaking and religating of one or both strands of the phosphodiester backbone of duplex DNA. TOP2β is a type II topoisomerase that induces double-strand DNA breaks at topologically associated domains (TADS) to relieve torsional stress arising during transcription or replication. TADS are anchored by CCCTC-binding factor (CTCF) and SMC1 cohesin proteins in complexes with TOP2β. Upon DNA cleavage, a covalent intermediate DNA-TOP2β (TOP2βcc) is transiently generated to allow for strand passage. The tyrosyl-DNA phosphodiesterase TDP2 can resolve TOP2βcc, but failure to do so quickly can lead to long-lasting DNA breaks. Given the role of CTCF/SMC1 proteins in the human papillomavirus (HPV) life cycle, we investigated whether TOP2β proteins contribute to HPV pathogenesis. Our studies demonstrated that levels of both TOP2β and TDP2 were substantially increased in cells with high-risk HPV genomes, and this correlated with large amounts of DNA breaks. Knockdown of TOP2β with short hairpin RNAs (shRNAs) reduced DNA breaks by over 50% as determined through COMET assays. Furthermore, this correlated with substantially reduced formation of repair foci such as phosphorylated H2AX (γH2AX), phosphorylated CHK1 (pCHK1), and phosphorylated SMC1 (pSMC1) indicative of impaired activation of DNA damage repair pathways. Importantly, knockdown of TOP2β also blocked HPV genome replication. Our previous studies demonstrated that CTCF/SMC1 factors associate with HPV genomes at sites in the late regions of HPV31, and these correspond to regions that also bind TOP2β. This study identifies TOP2β as responsible for enhanced levels of DNA breaks in HPV-positive cells and as a regulator of viral replication.

IMPORTANCE High-risk human papillomaviruses (HPVs) infect epithelial cells and induce viral genome amplification upon differentiation. HPV proteins activate DNA damage repair pathways by inducing high numbers of DNA breaks in both viral and cellular DNAs. This activation is required for HPV genome replication. TOP2β is a type II topoisomerase that induces double-strand DNA breaks at topologically associated domains (TADS) to relieve torsional stress arising during transcription or replication. Our studies demonstrate that TOP2β levels are increased in HPV-positive cells and that this is required for HPV replication. Importantly, our studies further show that knockdown of TOP2β reduces the number of breaks by over 50% in HPV-positive cells and that this correlates with substantially impaired activation of DNA repair pathways. This study identifies a critical mechanism by which HPV replication is regulated by the topoisomerase TOP2β through DNA break formation.

KEYWORDS CTCF, DNA damage, DNA replication, HPV, cohesin, topoisomerase

Human papillomaviruses (HPVs) infect stratified epithelia and link their productive life cycles to epithelial differentiation (1, 2). HPVs infect cells in the basal layer that

Citation Kaminski P, Hong S, Kono T, Hoover P, Laimins L. 2021. Topoisomerase 2β induces DNA breaks to regulate human papillomavirus replication. mBio 12:e00005-21. https://doi.org/10.1128/mBio.00005-21.

Editor Thomas Shenk, Princeton University

Copyright © 2021 Kaminski et al. This is an open-access article distributed under the terms of the Creative Commons Attribution 4.0 International license.

Address correspondence to Shiyuan Hong, hongshiyuan@cqmu.edu.cn, or Laimonis Laimins, l-laimins@northwestern.edu.

This article is a direct contribution from Laimonis A. Laimins, a Fellow of the American Academy of Microbiology, who arranged for and secured reviews by Karl Münger, Tufts University School of Medicine, and Elliot Androphy, Indiana University School of Medicine.

Received 7 January 2021
Accepted 11 January 2021
Published 9 February 2021

become exposed through microwounds and establish their double-stranded circular DNA genomes in the nucleus as low-copy-number episomes at 50 to 100 copies per cell. Productive viral replication or amplification occurs only in highly differentiated suprabasal cells and is dependent upon activation of the ataxia-telangiectasia mutated kinase (ATM) (3) as well as the ataxia-telangiectasia and RAD3-related kinase (ATR) pathways (4–6). These pathways are activated by the action of viral proteins, such as E6 and E7, alone and do not require viral replication (3–5). Previous studies have shown that activation of these pathways in HPV-positive cells occurs through induction of high levels of DNA breaks in both viral and cellular DNAs (7). The breaks in viral genomes are rapidly repaired by DNA damage repair pathways, and this is necessary for differentiation-dependent genome amplification (7). The mechanism by which HPV proteins induce high levels of DNA breaks, however, has not been clarified.

DNA breaks can be induced by exposure to exogenous DNA-damaging agents or through endogenous pathways such as through the action of topoisomerases. Topoisomerases regulate higher-order chromatin structures through the transient breaking and religation of one or both strands of the phosphodiester backbone of duplex DNA (8, 9). Type I topoisomerases (TOP1) cleave a single strand of duplex DNA, while type II topoisomerases (TOP2α and TOP2β) generate DNA double-strand breaks (DSBs) (9). TOP2α is expressed primarily in proliferating cells, while TOP2β is ubiquitously expressed, including during differentiation (8, 10). During breakage and religation by TOP2β, a covalent intermediate DNA-protein cross-link (TOP2βcc) is generated, which allows for strand passage and/or DNA unwinding to occur while the strand break remains bookmarked by the topoisomerase (11, 12). A certain proportion of TOP2βcc, however, result in long-lasting DNA breaks. These complexes can be resolved through the action of TDP2 enzymes (13) or the Mre11/RAD50/Nbs1 (MRN) complexes from the ATM pathway (14).

TOP2β cleavage of DNA is required for proper replication and transcription. Chromatin is arranged in DNA loops called topologically associated domains (TADS) which are anchored by CCCTC-binding factor (CTCF) factors in association with SMC1 cohesin proteins (15). TOP2β associates with CTCF and SMC1 at these anchor sites, and this is required to dissipate torsional stress arising from transcription or replication through the formation of DNA breaks (12, 16). Previous studies demonstrated that CTCF/SMC1 binding sequences are present in the late regions of almost all HPVs (17). Importantly, knockdown of either CTCF or SMC1 in HPV31-positive cells reduced viral transcription and blocked viral amplification (17). We therefore investigated whether TOP2β proteins played a role in regulating HPV pathogenesis and found that levels were increased in cells with high-risk HPV genomes, and this correlated with increased levels of DNA breaks. Notably, knockdown of TOP2β reduced the amount of DNA breaks by over 50%, which correlated with impaired activation of DNA damage repair pathways. Furthermore, HPV replication was also blocked following knockdown of TOP2β. Our studies identify a major source of DNA breaks in HPV-positive cells that is responsible for activation of DNA damage repair pathways and for regulation of viral replication.

RESULTS

Levels of TOP2β are increased in HPV-positive cells. To investigate whether TOP2β played a significant role in the HPV life cycle, we first examined the levels in cells that maintain either HPV16 or HPV31 episomes by Western blot analysis. The levels of TOP2β were found to be increased by approximately three- to fivefold in cells with HPV16 or HPV31 episomes (3) in comparison to human keratinocytes (Fig. 1A). HFK-16 and HFK-31 are stable cell lines that maintain viral episomes and were generated by transfection of human foreskin keratinocytes (HFKs) with recircularized viral genomes (18). CIN 612 cells maintain HPV31 episomes and were derived from a biopsy specimen of a cervical intraepithelial neoplasia 2 (CIN II) lesion (19). To investigate whether the levels of TOP2β changed upon differentiation, HPV-positive cells were

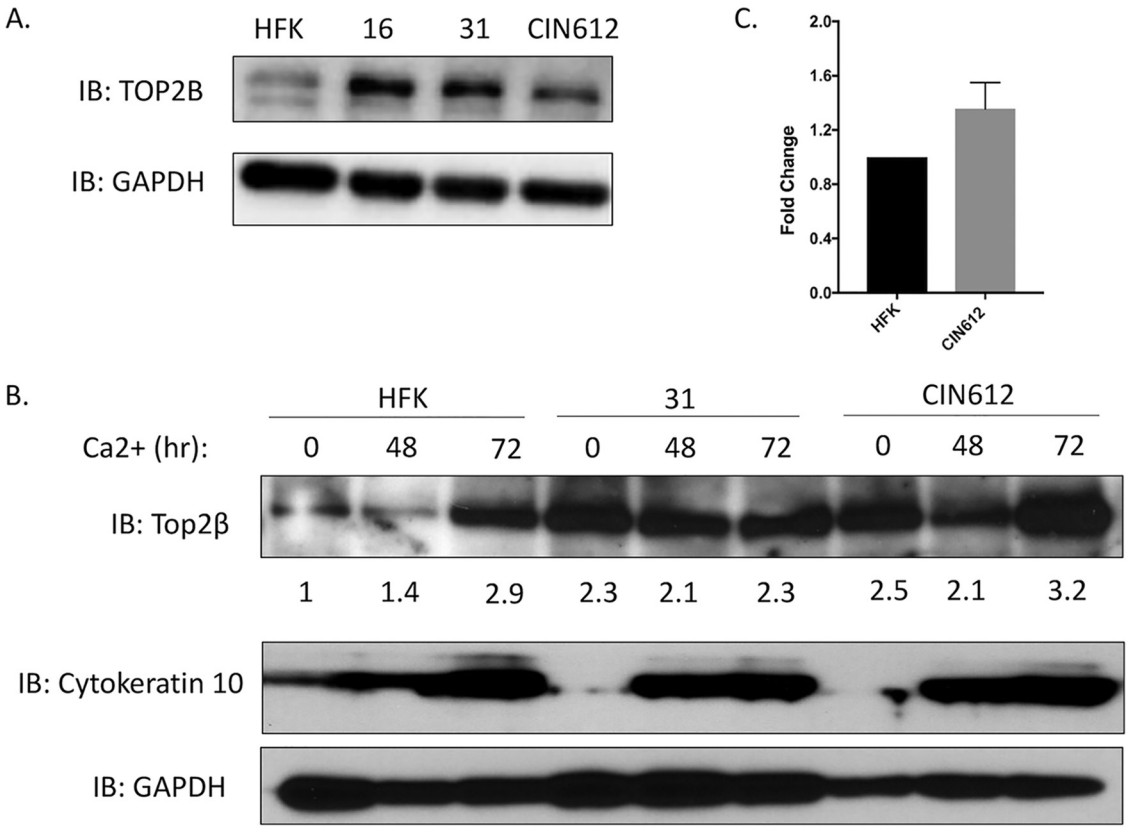

FIG 1 (A) TOP2β levels are increased in HPV-positive cells. Monolayer cultures of normal human foreskin keratinocytes (HFKs) along with cells with HPV episomes, HFK-16 (HPV16 positive), HFK-31 (HPV31 positive), and CIN 612 (HPV31 positive) cells, were examined by Western blot assay for levels of TOP2β. Glyceraldehyde-3-phosphate dehydrogenase (GAPDH) controls are shown below. Similar results were seen in three separate experiments. IB, immunoblotting. (B) TOP2β levels in HPV31-positive cells remain high upon differentiation in high-calcium media. HFK, HFK-31, and CIN 612 cells are shown at 48 and 72 h after calcium switch. Quantitation of band intensities is shown below the blot. Levels of differentiation marker cytokeratin 10 are shown along with GAPDH controls. (C). q-RT-PCR analysis of TOP2β transcripts in undifferentiated HFKs and CIN 612 cells.

induced to differentiate by the addition of high-calcium media and examined by Western blot analysis. Similar levels of TOP2β were observed in undifferentiated and differentiated HPV-positive cells. While HFKs exhibited low levels in undifferentiated cells as well as following 48 h of calcium-induced differentiation, an increase was consistently observed at 72 h of differentiation which is after amplification and late gene expression have been completed (Fig. 1B). The reason for this increase is unclear. We also investigated whether the increase of TOP2β in HPV-positive cells occurred at the level of transcription or posttranscriptionally. An analysis of TOP2β transcripts from undifferentiated HFKs and CIN 612 cells showed similar levels, indicating regulation occurred at the posttranscriptional level (Fig. 1C).

We next investigated whether replication of viral episomes or expression of viral proteins alone was responsible for inducing high levels of TOP2β. For this analysis, we infected HFKs with retroviruses expressing HPV16 or HPV31 E6, E7, or the combination of E6 and E7 and isolated stable cells. Examination of extracts from these cells by Western blot analysis demonstrated that E7 was largely responsible for increased levels of TOP2β (Fig. 2). The levels of TOP2β in E7-expressing cells were similar to those seen in cells that stably maintain viral episomes. We conclude that expression of E7 alone is sufficient to induce high levels of Top2β and that viral replication is not required.

Knockdown of TOP2β impairs HPV replication. To determine whether increased levels of TOP2β had an effect on viral functions, we examined the consequences of

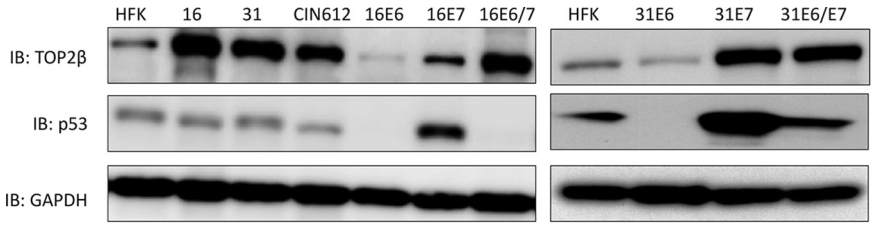

FIG 2 HPV E7 protein is responsible for increased levels of TOP2β. Western blot analysis of Top2β and p53 in the following cells: HFKs, HFK-16, HFK-31, CIN 612, HPV16 E6, HPV16 E7, HPV16 E6/E7, HPV31 E6, HPV31 E7, and HPV31 E6/E7. Cell lines expressing individual E6 or E7 proteins were generated by stable infection of HFKs with retroviral expression vectors expressing the various proteins. GAPDH loading control was included.

short hairpin RNA (shRNA) knockdowns on HPV replication. CIN 612 cells were first transiently infected with five individual lentiviruses expressing different shRNAs against TOP2β, and we identified two that had an effect. While expression of shRNA#3 resulted in a moderate suppression of TOP2β levels, shRNA#4 substantially reduced levels (Fig. 3). In addition, knockdown of TOP2β had no significant effect on differentiation, as indicated by expression of cytokeratin 10. Next, CIN 612 cells were infected with these two shRNAs, and stable lines were isolated and screened for the presence of viral episomes both in undifferentiated cells and following differentiation in high-calcium media for 72 h. As shown in Fig. 4, knockdown of TOP2β by either shRNA reduced the levels of viral episomes in undifferentiated cells. Screening for episomal genomes using an exonuclease V resistance assay that identifies circular genomes demonstrated a reduction of three- to fourfold in the levels of episomes in undifferentiated TOP2β knockdown cells (Fig. 4B). Since episomal templates are required for differentiation-dependent amplification, this process was also inhibited. In addition, knockdown of TOP2β had no effect on proliferation, as cell lines were passaged over 5 times in culture and grew similar to parental CIN 612 cells. Furthermore, early transcripts encoding E7 were detected using quantitative reverse transcription-PCR (q-RT-PCR) in both wild-type, control, and knockdown cells though levels were reduced by approximately 50% in the latter (Fig. 4C). These experiments indicate that TOP2β is a critical regulator of viral replication and may act in part through effects on HPV transcription.

TOP2β binds to HPV genomes at multiple sites. To begin to understand how TOP2β regulated HPV replication, we investigated whether TOP2β associated with viral genomes by performing chromatin immunoprecipitation analyses. For this study, several regions of the HPV31 genome were examined along with binding to cellular Alu sequences that were chosen as representative of cellular sequences. Alu sequences were chosen as they are highly transcribed and present in multiple copies. TOP2β was found to bind at high levels to the L2, E2 open reading frame (ORF), and E7 ORF

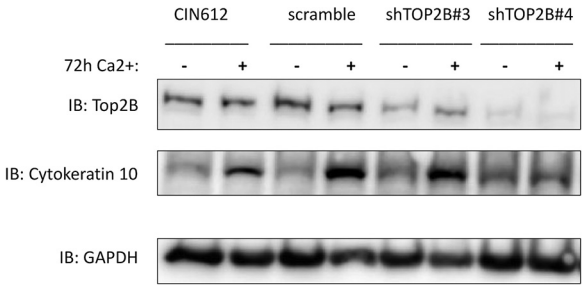

FIG 3 Identification of shRNA constructs that knock down or reduce TOP2β levels. Lentiviruses expressing either one of two shRNAs against TOP2β or a scramble control were generated in 293TT cells, and the resulting lentiviruses were used to infect CIN 612 cells. Following selection and expansion, stable cell lines were isolated. Following differentiation in high-calcium media for 0 or 72 h, cell extracts were examined for levels of TOP2β or cytokeratin 10 by Western blot analysis.

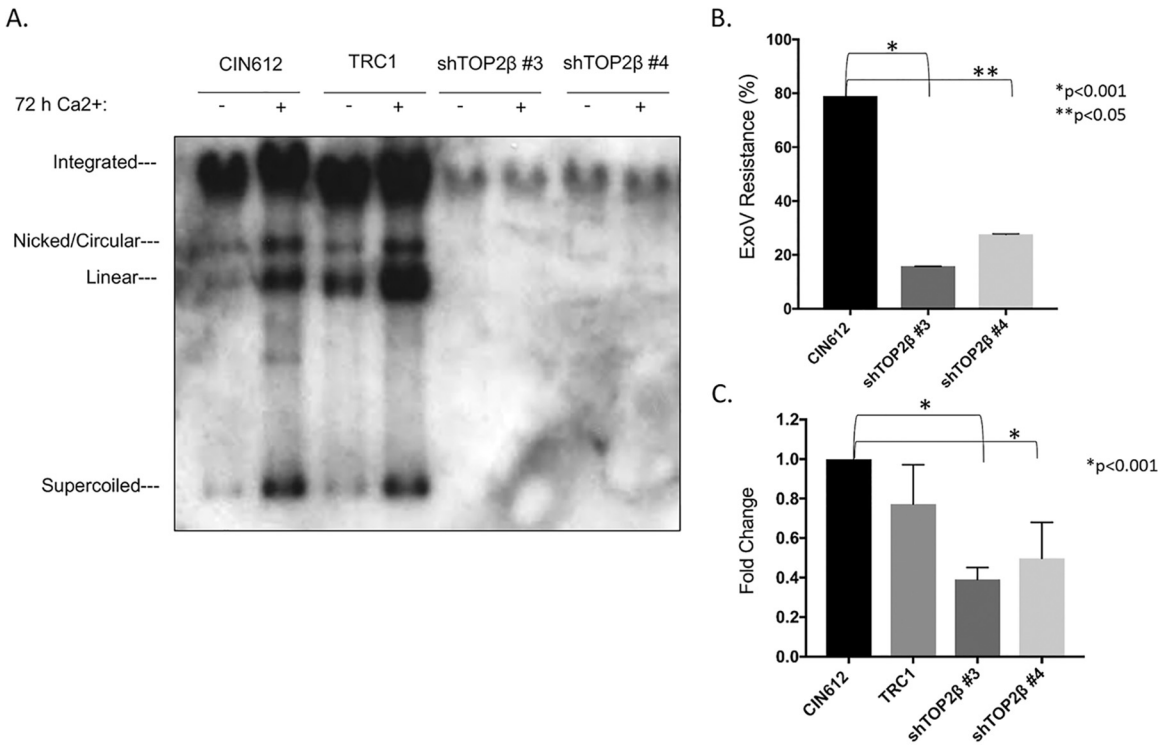

FIG 4 Knockdown of TOP2β in CIN 612 cells impairs stable maintenance of HPV31 episomes and amplification upon differentiation. (A) Southern blot analysis of CIN 612 wild-type and scramble control compared to cells with stable knockdown of TOP2β. Undifferentiated cells and cells after 72 of differentiation are shown. Supercoiled episomes, nicked circular, linear, multimers, and integrated genomes are indicated. (B) Exonuclease V (ExoV) analysis of episomal forms in undifferentiated CIN 612 cells and stable TOP2β knockdowns. Values that are statistically significantly different are indicated by bars and asterisks as follows: *, $P < 0.001$; **, $P < 0.05$. (C) q-RT-PC analysis of HPV early transcripts encoding E7 in undifferentiated cells. Parental CIN 612 cells, shRNA control TRC1-infected CIN 612 cells, and stable knockdowns of TOP2β in CIN612 background with shRNA #3 and shRNA #4 are shown. *, $P < 0.001$.

regions of the HPV genomes comparable to that detected at Alu sequences. In contrast, only a low level of TOP2β binding was detected at the upstream regulatory region (URR) of HPV31 (Fig. 5). Interestingly, the regions of the HPV31 genome that were found to bind TOP2β are those that contain putative or documented CTCF/SMC1 binding sites (17). No CTCF sites were identified in the URR that also fails to exhibit TOP2β binding. This suggests TOP2β associates with regions of the viral genomes that may be sites for CTCF/SMC1-mediated DNA looping.

High levels of TDP2 are present in HPV-positive cells. Previous studies have shown that the levels of DNA breaks in HPV-positive cells are two- to fivefold higher than in human keratinocytes (7). TOP2β can induce DNA breaks through the formation of TOP2βcc intermediates that are resolved through the action of the tyrosyl-DNA phosphodiesterase TDP2. TDP2 quickly resolves TOP2βcc allowing for religation of the DNA break. We investigated whether high levels of TOP2β correlated with increased amounts of TDP2. As shown in Fig. 6, TDP2 levels are increased by five- to sevenfold in cell lines that maintain episomes of HPV16 or HPV31, indicating that breaks induced by TOP2β can be rapidly resolved. We next investigated whether the increased amounts of TOP2β in HPV-positive cells also correlated with high levels of DNA breaks. To distinguish TOP2β-induced breaks from those caused by other mechanisms, we examined CIN 612 cell lines in which TOP2β levels were decreased by shRNAs with COMET assays. In COMET assays, single cells are suspended in agarose on glass slides followed by lysis, electrophoresis, and imaging by fluorescence (7). Large unbroken DNAs are retained in the nucleoid body, while broken DNAs migrate into the tail region. The levels of DNA breaks can be quantified by measuring the signal in the tail relative to that in the head. Examination of wild-type CIN 612 cells or those stably infected with

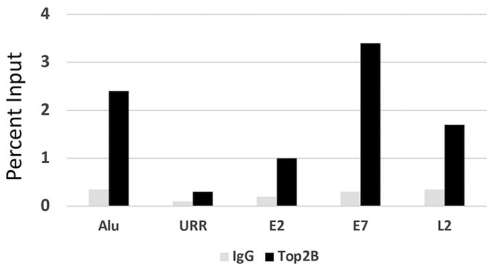

FIG 5 Chromatin immunoprecipitation analysis of TOP2β binding to regions on HPV31 episomes in comparison to Alu sequences. ChIP analyses were performed on monolayer cultures of CIN 612 cells. Similar results were observed in three independent experiments.

lentiviruses expressing a scrambled control shRNA demonstrated the presence of high levels of DNA breaks (Fig. 6B). In contrast, knockdown of TOP2β resulted in a statistically significant decrease in the amount of DNA breaks by approximately 50% to 60% (Fig. 6C).

Knockdown of TOP2β reduces nuclear foci containing DNA damage repair factors. Since the number of DNA breaks was reduced in HPV-positive cells upon TOP2β knockdown, we investigated whether this impacted the activation of DNA damage response (DDR) pathways. HPV activates both ATM and ATR factors and recruits these proteins to nuclear repair foci. To investigate whether DDR activation was altered by TOP2β knockdown, we examined whether there was a reduction in the number of cells with greater than three foci comparing wild-type CIN 612 cells to TOP2β knockdown cells. Immunofluoresence assays indicate that the number of cells with phosphorylated CHK1 (pCHK1)-, phosphorylated SMC1 (pSMC1)-, and phosphorylated H2Ax (γH2AX)-positive foci was reduced by 50% to 80% in knockdown cells (Fig. 7). Similarly, the levels of nuclear focus formation of other DDR factors, such as

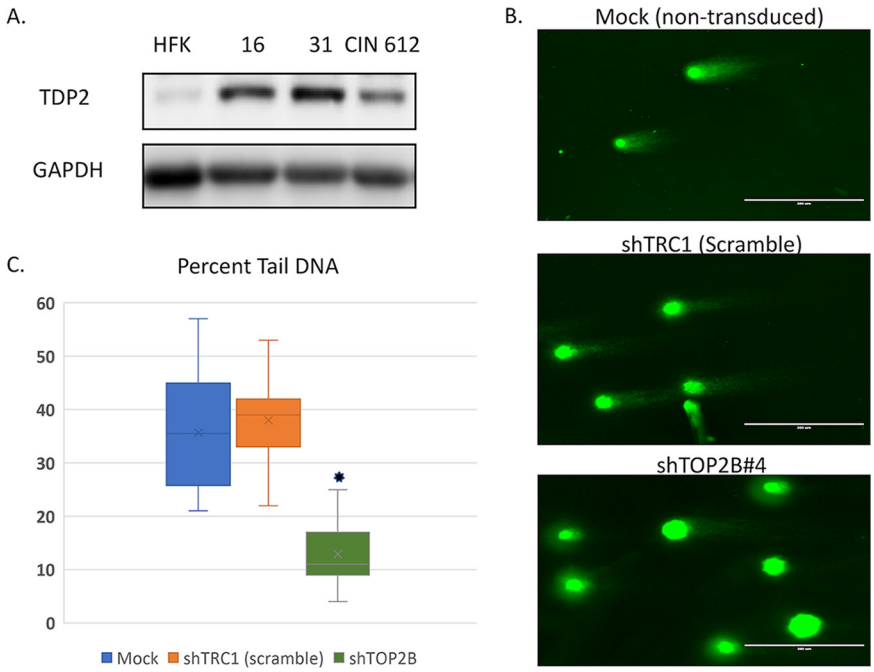

FIG 6 (A) TDP2 levels are increased in HPV-positive cells. Monolayer cultures of human foreskin keratinocytes (HFKs) along with cells with HPV episomes. HFK-16 (HPV16-positive), HFK-31 (HPV31-positive), and CIN 612 (HPV31-positive) cells were examined by Western blot assay for levels of TDP2. GAPDH controls are shown below. (B) Neutral COMET assays for DNA break formation in CIN 612 cells with mock, shTRC1 (scramble) and shRNA against TOP2β. Quantitation of percent tail versus nucleoid body is shown in the graph. A reduction in levels of DNA breaks of greater than 50% was detected in shRNA knockdown cells and is statistically significant. *, $P < 0.001$.

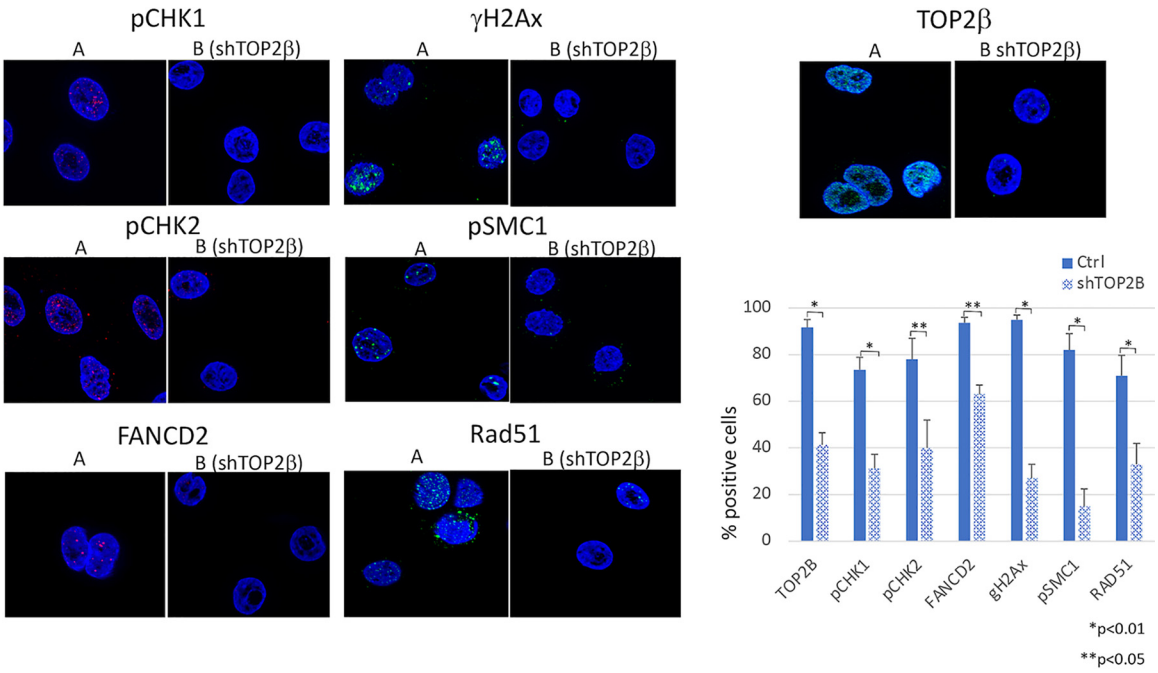

FIG 7 (A) Representative immunofluorescence staining of TOP2β and other DNA damage factors in CIN612 control and TOP2β knockdown cells. High magnification ($\times$63) is shown and indicates the presence of positive foci. (B) Comparative analysis of the percentages of cells that exhibited more than 3 focal localization of DDR factors between CIN 612 control cells and TOP2β knockdown cells. Ctrl, control. *, $P < 0.01$; **, $P < 0.05$.

pCHK2, FANCD2, and RAD51, were also reduced. TOP2β nuclear staining was present in a diffuse punctate pattern and reduced in knockdown cells. We conclude that TOP2β activity impacts the recruitment of DNA damage repair factors to foci consistent with the reduced numbers of breaks in the cells.

DISCUSSION

TOP2β relieves torsional stress caused by transcription and replication by inducing DNA breaks followed by religation (11, 16). Our studies indicated that TOP2β levels were elevated in HPV-positive cells by three- to fivefold which can lead to TOP2βcc-induced DNA breaks. Our studies further suggest that the increased expression of TOP2β was responsible for over half of the DNA breaks in HPV-positive cells and was important for the activation of DNA damage repair pathways. This is particularly significant in HPV-positive cells where activation of DNA damage repair pathways is necessary for HPV replication and differentiation-dependent amplification (7). Importantly, TOP2β was shown to be important for the stable maintenance of episomes as well as differentiation-dependent amplification which requires the presence of episomal genomes.

Topologically associated domains (TADS) are anchored through the binding of CTCF factors in association with SMC1 cohesin proteins and TOP2β. Previous studies demonstrated that CTCF/SMC1 factors associate with HPV genomes at conserved CTCF binding sites present in the late regions of all HPVs (17). Knockdown of either of these factors with shRNAs blocks HPV31 genome amplification and reduces late gene expression. The HPV31 L2, L1, and E2 ORFs contain consensus CTCF sequences and our recent 4C chromatin capture analyses demonstrated the formation of DNA loops between these sites as well as a putative cryptic site in the E7 ORF (K. Mehta, P. Hoover, and L. Laimins, unpublished results). No CTCF-directed looping was detected to sequences in the URR. In the present work, our TOP2β chromatin immunoprecipitation analyses showed TOP2β binding to these same four regions with no binding detected at the URR. This is consistent with TOP2β forming complexes with CTCF/SMC1 proteins at CTCF sites in HPV genomes. The Parish laboratory has shown that the CTCF site in

HPV18 E2 is critical for viral expression (20), and we have shown that knockdown of CTCF interferes with viral expression (17). These findings indicate that while TOP2β is responsible for global increases in DNA breaks in HPV-positive cells, it may have additional activities in directly regulating viral transcription and replication resulting from its binding to HPV genomes. The observation that expression of early viral genes was reduced by 50% upon stable knockdown of TOP2β is consistent with this hypothesis; however, many factors can influence viral expression in cells following integration of HPV genomes into host chromosomes. A more detailed analysis examining expression of all viral transcripts after transient knockdown of TOP2β is required for a more complete understanding. In addition, TOP2β or other topoisomerases may play a critical role in helping resolve concatemeric viral genomes resulting from amplification. Amplification has been reported to occur through several potential mechanisms, including a rolling circle type process or a novel unidirectional replication scheme involving multiple initiation sites (21, 22). It is also possible that amplification occurs though bidirectional theta structures. All three models require the action of topoisomerases such as TOP2β, TOP2α, or TOP1 to resolve concatemers. Interestingly, the Androphy lab has reported that E2 associated with TOP1 to facilitate its recruitment to viral episomes for replication and may also facilitate resolution of concatemers (23). TOP2β along with other topoisomerases may thus have multiple functions in regulating the HPV life cycle.

Along with increased amounts of TOP2β, high levels of the phosphodiesterase TDP2 (13), which rapidly resolves TOP2βcc structures, were also detected in HPV-positive cells. This suggests that once generated, TOP2βcc intermediates are rapidly resolved by TDP2, which is consistent with our previous observations that while DNA breaks are generated in viral genomes, they are rapidly repaired (7). Interestingly, TOP2βcc has been suggested to play a positive role in regulating pathogenesis of some viruses. Treatment of neurons with etoposide, which stabilizes TOP2βcc, results in increased expression of over 13 genes, particularly in the neuronal early response pathway as well as decreased expression of 300 other genes (24). Furthermore, high levels of TOP2βcc are induced in herpes simplex virus (HSV)-infected neurons, and these are needed for the maintenance of viral latency (25). Whether TOP2βcc structures contribute in a similar manner to the regulation of late HPV functions is an area for future study.

The results of our studies indicate that TOP2β is responsible for inducing many, but not all, DNA breaks in HPV-positive cells. The question arises as to what other mechanisms could be responsible for causing the other DNA breaks. One possibility is that TOP2α, which is highly homologous to TOP2β, could play a role. TOP2α is expressed primarily in cycling cells where it functions to relieve torsional stress resulting from replication and transcription (10). TOP2α also forms TOP2αcc covalent intermediates that result in DNA break formation (10). In contrast to TOP2β, TOP2α does not typically associate through CTCF/cohesin complexes but through less well-defined sequences. It is therefore likely that multiple endogenous pathways may contribute to DNA break formation in HPV-positive cells and that they play roles in regulating viral functions. Overall, our studies demonstrate critical roles for TOP2β in inducing DNA breaks and regulating the HPV life cycle.

MATERIALS AND METHODS

Cell culture and antibodies. Healthy human foreskin keratinocytes (HFKs) were isolated from deidentified neonatal specimens. HFK cells were transfected with HPV16 or HPV31 genomes to generate HFK-16 and HFK-31 cell lines that contain episomal HPV DNA as previously described (18). CIN 612 cells were isolated from a cervical cancer biopsy specimen and contain HPV31 episomes (19). All keratinocytes were cocultured in E-media with growth-arrested NIH 3T3 fibroblasts as described previously (3). Antibodies to phosphorylated CHK1 (pCHK1) (catalog no. 12302; Cell Signaling Technology [CST]), phosphorylated CHK2 (pCHK2) (catalog no. 2661; CST), FANCD2 (catalog no. 100182; Novus), phosphorylated H2Ax (γH2AX) (catalog no. 05636; Millipore), phosphorylated SMC1 (pSMC1) (catalog no. 4805S; CST), BRCA1 (catalog no. OP92; Millipore), RAD51 (catalog no. NB100148; Novus), and TOP2β (catalog no. A300-950A; Bethyl Laboratories) were used.

Calcium-induced differentiation. Keratinocytes were induced to differentiate through a calcium-mediated switch (3). Briefly, keratinocytes were plated at 5 million cells per 10-cm dish in M154 keratinocyte medium (Thermo Fisher) containing 0.07 mM Ca^{2+} and human keratinocyte growth serum (HKGS; Thermo Fisher). The next day, the medium was changed to 0.03 mM Ca^{2+} in M154 containing HKGS. After 24 h, the medium was changed once again to M154 containing 1.5 mM Ca^{2+} in the absence of HKGS. These cells were then incubated in high-calcium medium for 72 h to allow for proper differentiation.

Western blot analysis. For Western blot analysis of keratinocytes, cells were trypsinized from 10-cm plates, and the cell pellets were washed three times in cold phosphate-buffered saline (PBS). Cell pellets were then resuspended in an appropriate volume of radioimmunoprecipitation assay (RIPA) buffer for lysis and incubated on ice for 15 min to facilitate lysis. Lysates were then quantified using a Pierce BCA protein assay kit to determine the protein concentration of each sample. Lysates were then combined with 6× sodium dodecyl sulfate (SDS) protein loading buffer and passed through a 25-gauge (25G) syringe to homogenize lysates. Next, lysates were boiled at 100°C for 10 min to denature the samples. Samples were then centrifuged at 15,000 rpm for 1 min and then were either directly frozen or used for Western blot analysis. For each Western blot, 20 μg of protein was loaded into each well of a precast 10% polyacrylamide gel and run at 70 V for 2 h. Proteins were then transferred onto a polyvinylidene difluoride (PVDF) membrane using wet transfer apparatus at 400 mA for 90 min at 4°C. The membrane was then blocked in 5% nonfat milk in TBST (Tris, NaCl, Tween) on a rotating platform at room temperature for 1 h. Primary antibodies were then added to TBST, and membranes were incubated overnight on a rotating platform at 4°C. The following day, membranes were washed three times with TBST for 5 min each and were incubated with secondary antibodies conjugated with horseradish peroxidase (HRP) for 1 h at room temperature. After an additional three washes in TBST, membranes were activated using ECL blotting substrate, and bands were visualized using a LICOR imaging station.

Neutral COMET assay. Cells were seeded onto glass slides suspended in low-melting-point agarose, lysed, and electrophoresed according to manufacturer's instructions (Trevigen Comet assay [ESII system]). Comets were visualized using a Zeiss Axioscope, and the percent tail DNA was quantitated using open source software OpenComet for FIJI.

Southern blot analysis. Keratinocytes were first washed three times in room temperature PBS and then trypsinized from 10-cm plates and transferred to 15-ml conical tubes. Cells were then pelleted and washed in PBS. Cell pellets were resuspended in 3 ml Southern lysis buffer. To each sample, RNase A was added to a final concentration of 50 μg/ml and incubated at room temperature for 15 min. Next, SDS was added to a final concentration of 0.2% along with proteinase K to a final concentration of 50 μg/ml, and samples were incubated overnight at 37°C. The next day, samples were passed through an 18G syringe five times, and DNA was extracted using phenol-chloroform/isoamyl alcohol-based extraction. Following extraction, DNA was precipitated by adding 6 ml of 100% ethanol to each sample, and the samples were incubated overnight at −20°C. The following day, precipitated DNA was pelleted by centrifugation at 5,000 rpm for 30 min at 4°C. DNA pellets were then washed three times in 70% ethanol and were then air dried before resuspension in Tris-EDTA (TE) buffer. DNA was quantified using a nanodrop UV spectrophotometer. For each sample, 5 μg of DNA was digested using XhoI restriction enzyme. Digested DNA was separated on a 0.8% agarose gel at 40 V for 16 h. DNA was depurinated by washing the gel in HCl, followed by neutralization in NaOH and transferred onto a nylon membrane using a vacuum apparatus. Transferred DNA was then neutralized in 2× sodium citrate buffer (SCC) and UV cross-linked to the nylon membrane. The membrane was then equilibrated in a prehybridization buffer before the addition of ^{32}P-labeled HPV31 DNA probe. Following addition of radiolabeled probe, the membrane was incubated overnight and washed in SCC the following day. After the DNA bands were washed, the DNA bands were visualized using autoradiography film.

Exonuclease V assay. Episomal DNA was measured using an exonuclease V assay described by the Sapp lab (26). Total DNA was isolated from cells using phenol-chloroform followed by precipitation with ethanol. DNA was then quantitated using Qubit 4 fluorometer with the BR DNA assay kit (Invitrogen), and 1 μg of DNA was digested using the exonuclease V. DNA was then purified using GeneJet PCR purification (Thermo Fisher) and amplified with Roche light cycler 480 using primers specific to E7. The forward primer was 5′-ATGAGCAATTACCCGACAGCTCAGA, and the reverse primer was 5′-AGACTTACACTGACAACAAAAGGTAACGAT.

q-RT-PCR for E7 and TOP2β transcripts. Total RNA was isolated from lysed cells using an EZ-10 spin column total RNA minipreps super kit (Bio Basic) following the manufacturer's instructions. RNA was then digested with DNase I and purified again through RNA mini prep kit again. cDNA was made using a high-capacity RNA-to-cDNA kit (Applied Biosystems) following the manufacturer's instructions. cDNA was quantitated using a Qubit 4 fluorometer with a single-stranded DNA (ssDNA) assay kit (Invitrogen). Quantitative reverse transcription-PCRs (qRT-PCRs) were performed using primers specific to E7 or TOP2b with a Roche light cycler 480. For E7, the forward primer was 5′-ATGAGCAATTACCCGACAGCTCAGA and the reverse primer was 5′-AGACTTACACTGACAACAAAAGGTAACGAT (IDT). For Top2β, the forward primer was 5′CAGCCCGAAAGACCTAAATAC, and the reverse primer was 5′-ATCTAACCCATCTGAAGGAAC. The primers were obtained from Sigma-Aldrich.

Chromatin immunoprecipitation (ChIP)-qPCR. Keratinocytes were fixed in 1% formaldehyde in PBS for 5 min. Cells were then scraped from 10-cm dishes and washed three times in cold PBS. Fixed cells were then lysed by resuspending cells in 500 μl of RIPA buffer on ice. Lysates were sonicated in 100-μl aliquots using a 30-s-on/90-s-off cycle for 20 min on high output. Sonicated lysates were then stored at −80°C. Protein G beads were added and precleared overnight on a rotating platform using 0.5 mg/ml bovine serum albumin (BSA) and 0.5 mg/ml salmon sperm in PBS. The following morning,

beads were magnetically separated, and 2 μg of antibody was added to each immunoprecipitation (IP) reaction followed by incubation for 8 h at 4°C on a rotator. Next, the beads were magnetically separated, and 100 μl of sonicated cell lysate was added to each reaction mixture along with 900 μl of RIPA buffer. IP reaction mixtures were then incubated overnight at 4°C on a rotator. The following day, IP reactions were magnetically separated, and the beads were washed eight times in ice-cold RIPA buffer. To elute captured DNA/protein, the beads were resuspended in an elution buffer (5 mM EDTA, 1% SDS, 50 mM Tris [pH 7.5], 50 mM NaCl) and incubated for 30 min at 55°C with shaking. The beads were then separated by centrifugation at 15,000 $\times$ *g*, and the supernatant was moved to a clean Eppendorf tube. The eluted fractions were next reverse cross-linked at 55°C overnight. Immunoprecipitated DNA was then purified using standard Qiagen quick purification columns. DNA was quantified by qPCR using primers specific to HPV genomes as well as Alu repeat sequences specific to human genomic DNA. The relative amount of specific DNA per sample was normalized to an input chromatin fraction that did not undergo immunoprecipitation.

Immunofluorescence, microscopy, and ImageJ analysis. Cells were grown on treated coverslips under media. Prior to analysis, the cells were fixed with 4% paraformaldehyde, permeabilized in PBS with Triton X-100 (PBST), blocked with normal goat serum (NGS), and probed with primary antibodies in NGS at 4°C overnight. After three washes in PBST, the slides were incubated with secondary antibodies, followed by 4′,6′-diamidino-2-phenylindole (DAPI) incubation, and coverslips were mounted. Images were taken on a Zeiss Axioscope, and the data were imported into ImageJ for analysis. The percentage of positive-staining cells was evaluated by comparing the number of cells with nuclear focal staining to the total number of cells as determined by DAPI staining, and greater than 20 cells were examined in each group.

Statistical analysis. IBM SPSS Statics24 software was used for statistical analysis. Comparison between two groups was performed with unpaired Student's *t* test. *P* values of <0.05 were considered to be statistically significant.

ACKNOWLEDGMENTS

L.L. was supported by grants from the National Cancer Institute (RO1CA059655 and RO1CA142861).

We thank Elona Gusho for help with analysis and figures.

REFERENCES

1. Moody CA, Laimins LA. 2010. Human papillomavirus oncoproteins: pathways to transformation. Nat Rev Cancer 10:550–560. https://doi.org/10.1038/nrc2886.
2. zur Hausen H. 2009. Human papillomavirus & cervical cancer. Indian J Med Res 130:209.
3. Moody CA, Laimins LA. 2009. Human papillomaviruses activate the ATM DNA damage pathway for viral genome amplification upon differentiation. PLoS Pathog 5:e1000605. https://doi.org/10.1371/journal.ppat.1000605.
4. Hong S, Cheng S, Iovane A, Laimins LA. 2015. STAT-5 regulates transcription of the topoisomerase IIβ-binding protein 1 (TopBP1) gene to activate the ATR pathway and promote human papillomavirus replication. mBio 6:e02006-15. https://doi.org/10.1128/mBio.02006-15.
5. Anacker DC, Aloor HL, Shepard CN, Lenzi GM, Johnson BA, Kim B, Moody CA. 2016. HPV31 utilizes the ATR-Chk1 pathway to maintain elevated RRM2 levels and a replication-competent environment in differentiating keratinocytes. Virology 499:383–396. https://doi.org/10.1016/j.virol.2016.09.028.
6. Edwards TG, Vidmar TJ, Koeller K, Bashkin JK, Fisher C. 2013. DNA damage repair genes controlling human papillomavirus (HPV) episome levels under conditions of stability and extreme instability. PLoS One 8:e75406. https://doi.org/10.1371/journal.pone.0075406.
7. Mehta K, Laimins L. 2018. Human papillomaviruses preferentially recruit DNA repair factors to viral genomes for rapid repair and amplification. mBio 9:e00064-18. https://doi.org/10.1128/mBio.00064-18.
8. Austin CA, Lee KC, Swan RL, Khazeem MM, Manville CM, Cridland P, Treumann A, Porter A, Morris NJ, Cowell IG. 2018. TOP2B: the first thirty years. Int J Mol Sci 19:2765. https://doi.org/10.3390/ijms19092765.
9. Harper JW, Elledge SJ. 2007. The DNA damage response: ten years after. Mol Cell 28:739–745. https://doi.org/10.1016/j.molcel.2007.11.015.
10. Thakurela S, Garding A, Jung J, Schubeler D, Burger L, Tiwari VK. 2013. Gene regulation and priming by topoisomerase IIalpha in embryonic stem cells. Nat Commun 4:2478. https://doi.org/10.1038/ncomms3478.
11. Canela A, Maman Y, Huang SN, Wutz G, Tang W, Zagnoli-Vieira G, Callen E, Wong N, Day A, Peters JM, Caldecott KW, Pommier Y, Nussenzweig A. 2019. Topoisomerase II-induced chromosome breakage and translocation is determined by chromosome architecture and transcriptional activity. Mol Cell 75:252–266.e8. https://doi.org/10.1016/j.molcel.2019.04.030.
12. Canela A, Maman Y, Jung S, Wong N, Callen E, Day A, Kieffer-Kwon KR, Pekowska A, Zhang H, Rao SSP, Huang SC, McKinnon PJ, Aplan PD, Pommier Y, Aiden EL, Casellas R, Nussenzweig A. 2017. Genome organization drives chromosome fragility. Cell 170:507–521.e18. https://doi.org/10.1016/j.cell.2017.06.034.
13. Gomez-Herreros F, Zagnoli-Vieira G, Ntai I, Martinez-Macias MI, Anderson RM, Herrero-Ruiz A, Caldecott KW. 2017. TDP2 suppresses chromosomal translocations induced by DNA topoisomerase II during gene transcription. Nat Commun 8:233. https://doi.org/10.1038/s41467-017-00307-y.
14. Fagan-Solis KD, Simpson DA, Kumar RJ, Martelotto LG, Mose LE, Rashid NU, Ho AY, Powell SN, Wen YH, Parker JS, Reis-Filho JS, Petrini JHJ, Gupta GP. 2020. A p53-independent DNA damage response suppresses oncogenic proliferation and genome instability. Cell Rep 30:1385–1399.e7. https://doi.org/10.1016/j.celrep.2020.01.020.
15. Gosalia N, Neems D, Kerschner JL, Kosak ST, Harris A. 2014. Architectural proteins CTCF and cohesin have distinct roles in modulating the higher order structure and expression of the CFTR locus. Nucleic Acids Res 42:9612–9622. https://doi.org/10.1093/nar/gku648.
16. Uuskula-Reimand L, Hou H, Samavarchi-Tehrani P, Rudan MV, Liang M, Medina-Rivera A, Mohammed H, Schmidt D, Schwalie P, Young EJ, Reimand J, Hadjur S, Gingras AC, Wilson MD. 2016. Topoisomerase II beta interacts with cohesin and CTCF at topological domain borders. Genome Biol 17:182. https://doi.org/10.1186/s13059-016-1043-8.
17. Mehta K, Gunasekharan V, Satsuka A, Laimins LA. 2015. Human papillomaviruses activate and recruit SMC1 cohesin proteins for the differentiation-dependent life cycle through association with CTCF insulators. PLoS Pathog 11:e1004763. https://doi.org/10.1371/journal.ppat.1004763.
18. Frattini MG, Lim HB, Laimins LA. 1996. *In vitro* synthesis of oncogenic human papillomaviruses requires episomal genomes for differentiation-dependent late expression. Proc Natl Acad Sci U S A 93:3062–3067. https://doi.org/10.1073/pnas.93.7.3062.
19. Meyers C, Frattini M, Hudson J, Laimins L. 1992. Biosynthesis of human papillomavirus from a continuous cell line upon epithelial differentiation. Science 257:971–973. https://doi.org/10.1126/science.1323879.
20. Pentland I, Campos-Leon K, Cotic M, Davies KJ, Wood CD, Groves IJ, Burley M, Coleman N, Stockton JD, Noyvert B, Beggs AD, West MJ,

Roberts S, Parish JL. 2018. Disruption of CTCF-YY1-dependent looping of the human papillomavirus genome activates differentiation-induced viral oncogene transcription. PLoS Biol 16:e2005752. https://doi.org/10.1371/journal.pbio.2005752.

21. Orav M, Gagnon D, Archambault J. 2019. Interaction of the human papillomavirus E1 helicase with UAF1-USP1 promotes unidirectional theta replication of viral genomes. mBio 10:e00152-19. https://doi.org/10.1128/mBio.00152-19.
22. Orav M, Geimanen J, Sepp EM, Henno L, Ustav E, Ustav M. 2015. Initial amplification of the HPV18 genome proceeds via two distinct replication mechanisms. Sci Rep 5:15952. https://doi.org/10.1038/srep15952.
23. Thomas Y, Androphy EJ. 2019. Acetylation of E2 by P300 mediates topoisomerase entry at the papillomavirus replicon. J Virol 93:e02224-18. https://doi.org/10.1128/JVI.02224-18.
24. Madabhushi R, Gao F, Pfenning AR, Pan L, Yamakawa S, Seo J, Rueda R, Phan TX, Yamakawa H, Pao PC, Stott RT, Gjoneska E, Nott A, Cho S, Kellis M, Tsai LH. 2015. Activity-induced DNA breaks govern the expression of neuronal early-response genes. Cell 161:1592–1605. https://doi.org/10.1016/j.cell.2015.05.032.
25. Hu HL, Shiflett LA, Kobayashi M, Chao MV, Wilson AC, Mohr I, Huang TT. 2019. TOP2beta-dependent nuclear DNA damage shapes extracellular growth factor responses via dynamic AKT phosphorylation to control virus latency. Mol Cell 74:466–480.e4. https://doi.org/10.1016/j.molcel.2019.02.032.
26. Myers JE, Guidry JT, Scott ML, Zwolinska K, Raikhy G, Prasai K, Bienkowska-Haba M, Bodily JM, Sapp MJ, Scott RS. 2019. Detecting episomal or integrated human papillomavirus 16 DNA using an exonuclease V-qPCR-based assay. Virology 537:149–156. https://doi.org/10.1016/j.virol.2019.08.021.